J Therm Anal Calorim (2010) 102:403–412
DOI 10.1007/s10973-010-0947-x

Crystallization of polymers

A personal view on a lifetime in research

Vincent B. F. Mathot

NATAS2009 Special Issue
© Akadémiai Kiadó, Budapest, Hungary 2010

Abstract In the past 35 years, the emphasis of the activities has been doing and stimulating of fundamental research; managing research toward improvement and development of polymer systems and industrial applications of polymers; and providing analytical support by utilization and development of characterization techniques and methods. Throughout, the research activities concerned the study of molecular structure, crystallization and melting, morphology, and thermal properties of polymeric systems, and to study and understand the relations between these topics. With respect to Thermal Analysis & Calorimetry (TA&C), quantitative research has been realized in the field of crystallization of polymers of which a choice of recent work is discussed.

Keywords Reorganization · Recrystallization · Crystallization · Cold crystallization · Fast scanning calorimetry · High performance DSC (HPer DSC) · Water · Droplet dispersion · Homogeneous nucleation · Poly-L-lactic acid · Polyamide · Polypropylene · Polyethylene · Ethylene copolymer

V. B. F. Mathot (✉)
SciTe B.V, Ridder Vosstraat 6, 6162 AX Geleen, The Netherlands
e-mail: vincent.mathot@scite.nl; vincent.mathot@gmail.com

V. B. F. Mathot
Division of Molecular and Nanomaterials, Department of Chemistry, Katholieke Universiteit Leuven, Celestijnenlaan 200F, Heverlee 3001, Belgium

Introduction

In the past 35 years, the emphasis of the activities has been doing and stimulating of fundamental research at DSM Research and (for a decade) at the Katholieke Universiteit Leuven, Belgium [with B. Goderis, G. Groeninckx, H. Reynaers]; to manage research at DSM toward improvement and development of polymers and toward industrial applications; and to provide analytical support. Since 2003, activities are also continued through SciTe B.V., short for Science & Technology, which is a Small and Medium Enterprise. Throughout, the research activities concerned molecular structure, crystallization and melting, morphology, and thermal properties of polymeric systems.

With respect to Thermal Analysis & Calorimetry (TA&C), quantitative research—triggered by the pioneering work of A. Gray, M. Richardson and B. Wunderlich—has been realized over more than three decades [with S. de Boer, L. Dirks, M. Pijpers, J. van Ruiten, R. Scherrenberg, J. Smeets, E. van der Vegte] within the central TA&C group of DSM Research, providing an output [by typically four Full-Time Equivalents (FTEs)] for the main technique—DSC—of typically 12,000 high-quality curves with interpretations a year.

One class of polymers where the unraveling of the molecular structure has benefitted substantially from TA&C has been the polyolefins [1], for example heterogeneous ethylene copolymers like linear low-density polyethylene (LLDPE) and very low-density polyethylene (VLDPE). In combination with appropriate (cross) fractionation methods [A. Brands, W. Bunge, N. Meierink, H. Schoffeleers], both molecular structure and morphology [R. Deblieck] were clarified at a very early stage (1984), because knowledge resulting from earlier fundamental studies in the field on linear polyethylene (LPE), high-

density polyethylene (HDPE), low-density polyethylene (LDPE), ultra high molar mass polyethylene or ultra high-molecular-weight polyethylene (UHMWPE), and ethylene-based (E..) copolymers was already built up. From the start of the research on copolymer [H. Suzuki] crystallization [F. Balta Calleja, P. van Ekeren, S. Vanden Eynde, A. Flores, U. Gedde, M. Hedenqvist, G. Höhne, T. Madkour G. Michler, C. van Miltenburg, B. Neway, M. Peeters, J. Schawe] has been a topic. Starting with the theories by Flory and Kilian, the proper background based on thermodynamics for in-depth studies was obtained, which led to an adaption of the Flory theory (which was approved by him) for crystallites having finite lateral dimensions as in practice [still unpublished]. This was a first step toward studies under realistic conditions, and it linked up with another realistic approach, the cold crystallization theory by Wunderlich. Because kinetics usually overrules thermodynamics; nowadays the best results are obtained by dynamic Monte Carlo simulation of crystallization, melting, and morphology, resulting in a series of papers on crystallization [D. Frenkel, W. Hu]. Excitingly, it was even possible to calculate DSC- and crystallinity curves of copolymers, both in cooling and heating, showing the well-known hysteresis related to supercooling. The input needed—realistic copolymer chains—led also to establishing the 'missing link' between polymerization [N. Friederichs, D. Joubert, W. Kaminsky, C. Piel, B. Wang] and the resulting molecular structure by modeling [Ch. Fabrie, E. Karssenberg, T. Tiemersma, T. Zwartkruis] of state-of-the-art whole NMR spectra [P. Adriaensens, J. Gelan, G. van der Velden].

A study [2] on dynamic crystallization of LPE and into determination of a realistic-free enthalpy (Gibbs-free energy) change function or $\Delta g(T)$, the driving force for crystallization, coincided with the development of the Regime theory by Hoffman. Especially Regime III was of interest for industry because it described nucleation and growth at high supercoolings, like under processing conditions. Hoffman was aware of the fact that the driving force, used in all crystallization theories, was temperature dependent. Therefore, for large supercoolings he proposed various approximations, the best known being a modification of the approximation normally used, $\Delta g(T) = \Delta h(T_m)\Delta T/T_m$, into $\Delta g(T) = \Delta h(T_m)\Delta T/T_m \cdot T/T_m$, which was in fact a best guess at the time (1958). It was shown [2, 3] that nowadays such approximations have to be replaced by the $\Delta g(T)$ as based on experimental (specific) heat capacity, $c_p(T)$, data. In general, functions like $\Delta c_p(T)$, $\Delta h(T)$, $\Delta s(T)$, $\Delta g(T)$—named reference differential functions—are obtained by subtracting the so-called reference functions for the extreme states of matter in case the two-state model applies [4], meaning that molecules are thought to be in one of two states: in the liquid (amorphous or melt) state or in the solid (crystalline or glass) state, represented by the reference functions of the extreme states possible (as usually indicated by indices a and c, respectively): $c_{pa}(T)$; $h_a(T)$; $s_a(T)$; $g_a(T)$ and $c_{pc}(T)$; $h_c(T)$; $s_c(T)$; $g_c(T)$, respectively. These reference functions and the reference differential functions like the reference differential-free enthalpy (Gibbs-free energy) function or driving force $\Delta g(T) = g_a(T) - g_c(T)$ nowadays can be obtained via the ATHAS databank [M. Pyda, B. Wunderlich]. Other reference differential functions are of interest too, like, for example, $\Delta h(T)$: the temperature-dependent enthalpy of transition [or heat of melting ('fusion')/crystallization]: it is not a constant value.

Applying this thermodynamic background, one can utilize the concept further by comparing the results of a quantitative experiment, either $c_p(T)$ or dq/dT (q stands for Q/m, the specific heat), with the reference functions. Firstly, this enables to judge the quality of the experiment. Secondly, it permits to determine interesting functions like the crystallinity as function of temperature, $w_c(T)$, as well as the basis-line $c_{pb}(T)$ and the excess $c_{pe}(T)$. A topic still not completely addressed is the use of a three-state model in case of a Rigid Amorphous Fraction [J. van Ruiten]. Such a study should preferably be combined with other techniques, like dielectric spectroscopy [A. de Rooij, J. Tacx, J. van Turnhout, M. Wübbenhorst] and especially X-ray and solid-state NMR, because only then a full-morphological model can be constructed [M. Basiura, W. Bras, J. Janicki, M. Koch, V. Litvinov, S. Rabiej, T. Ryan, R. Scherrenberg, C. Vonk, M. Wevers].

With regard to industrial utilization of TA&C [5–9], the applicability of new techniques to polymeric systems, like temperature-modulated DSC and TM reaction calorimetry [A. van Hemelrijck, R. Scherrenberg, P. Steeman, E. van der Vegte], and scanning thermal microscopy [H. Pollock, R. Smallwood] have been scrutinized. A break-through was realized by the development and application of high performance DSC (HPer DSC) [M. Pijpers, G. Vanden Poel], as followed by its commercial equal: the HyperDSC of Perkin-Elmer. This development is part of a move toward exploration of fast scanning calorimeters (FSC), with exponents like the recently introduced RHC of TA Instruments and especially the Fast Scanning (chip) Calorimeter [C. Schick, R. Tol]. The rationale for this development is that, in practice, quite some processes occur at much higher rates than realizable using Standard DSC and, secondly, most materials and substances, including polymers and pharmaceuticals, are in metastable states. Thermal history—specifically cooling and heating rates—and sample/product treatment can change their behavior drastically, influencing end properties. Phenomena related to metastability are well known to polymer scientists; daily they encounter super cooling, amorphization, 'hot'

crystallization, cold crystallization, recrystallization (after melting), annealing, etc. In addition, among the many advantages of HPer DSC, measuring on minute amounts—down to the microgram level—of materials is possible, like yields of fractionations [R. Brüll, I. Garcia, L-C. Heinz, A. Krumme, N. Luruli, H. Pasch].

Heterogeneous-, fractionated-, and homogeneous nucleation in case of polymer blends and composites [W. Bruls, D. Homminga, M. Salmerón Sánchez] have become topics for research linking up with studies on confined crystallization [R. Tol]. Crystallization at much lower temperatures than usual is realized in case of sub-micrometer dispersions, and homogenous nucleation is found to happen even without applying fast-cooling methods. Recently, routes for polymer systems have been set up which are 'green,' e.g., working with water as a medium for polymer dispersions and as a solvent. Thus, very stable water-borne dispersions of homogeneous ethylene-1-octene (EO) copolymers and of maleic anhydride-grafted polypropylenes (PP-*g*-MA) were prepared [L. Bremer, J. Ibarretxe Uriguen]. As in case of the blends mentioned, again particles having sizes down to sub-micrometer scale were generated in a controlled way and in large quantities. Thus, the lowest crystallization peak temperature and the largest extra supercooling ever observed for PP in analogous experiments, 33 and 77 °C, respectively, were realized. As another example, based on an in-house DSM study in 1995, fast and full dissolution of polyamide (PA) in water can be realized [K. Charlet, J. Devaux, M. Wevers]. It drastically lowers the temperature of subsequent crystallization and melting: depressions of 60 to 100 °C have been measured.

A few of the recent developments sketched [10] are briefly discussed in this article.

Results and discussion

Fast scanning calorimetry

As hinted at in the "Introduction" section, studying crystallization of real polymers under realistic conditions is of importance, not only for industry but also from a scientific point of view, because it provides an opportunity to arrive at the opposite of thermodynamic equilibrium conditions. Thus, one has to deal with the dynamics of processes occurring which is a challenging topic in itself. In order to approximate conditions of equilibrium, cooling at extremely slow rates, in combination with annealing procedures, has been applied in the past, also in order to obtain samples with high crystallinity. By contrast, it would be beneficial for the understanding of (in)capabilities of chains to crystallize or even amorphize, by cooling them at extremely high cooling rates. In practice one can find analogous situations and everything in between the extremes. Experimentally it is a challenging and very demanding job to realize fast, controlled cooling at constant rates. In addition, also fast heating is of interest in order to hinder or even suppress phenomena like reorganization, recrystallization, and cold crystallization during heating, solid–solid transitions; to study superheating, etc. If one can overcome the difficulties, the benefits are substantial, as it is well known that thermal history—specifically cooling and heating rates—and sample/product treatment can change the behavior of polymer products drastically, influencing end properties. Thus, the challenge is to realize scan rates higher than typical rates of Standard DSC, which are centered on approximately 10 °C min^{-1}.

The development of FSC

In the past decade this challenge has been met by realization of breakthroughs via the development of various FSC. One of the highlights was the introduction of HPer DSC (high performance meaning higher scan rates and still quantitative operation) [11–13] (see Fig. 1). It has been promoted commercially since then by Perkin-Elmer (the HyperDSC, up to 750 °C min^{-1} [14]) and recently also by TA Instruments (the RHC, up to 2000 °C min^{-1}) [15]. Another breakthrough was the development of extremely fast operating chip-calorimeters, as described in papers by Allen et al. and by Schick et al., see e.g., [16, 17] and references therein.

Figure 2 shows for a PP sample one of the great benefits of HPer DSC [18]: it can mimic most of the cooling rates used in processing. Increasing the cooling rate has a drastic influence on the way of crystallization of polymers: it occurs at lowered temperatures while the peak area of crystallization is decreased, meaning that the crystallinity goes down. Depending on their crystallizability some

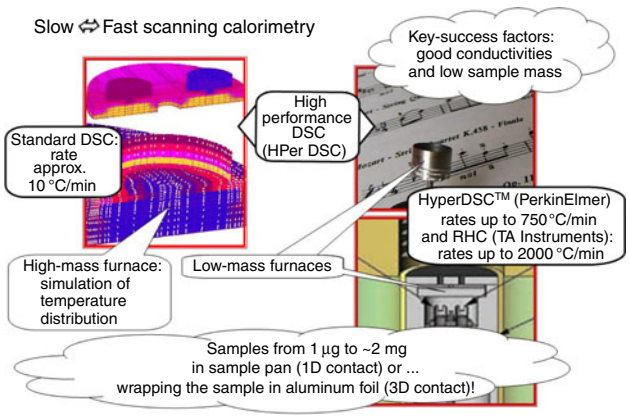

Fig. 1 The development of HPer DSC, complementary to Standard DSC, by improving crucial thermal conductivity paths, including thermal contact between sample container and sample; decreasing of the sample mass with increasing scan rate; miniaturization of the sample container, etc.

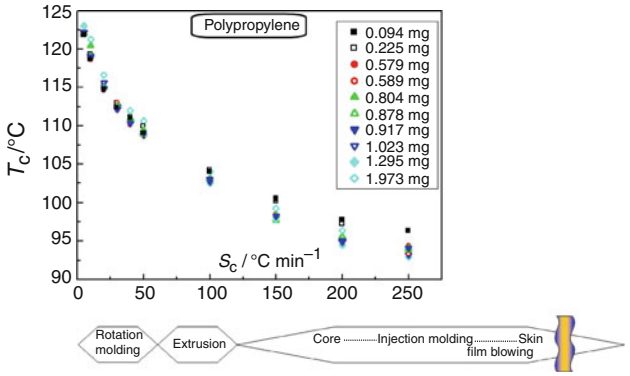

Fig. 2 Peak maximum crystallization temperatures from DSC cooling curves, as function of cooling rate and for various sample masses for a PP, which rates are compared with the cooling rate ranges covered by the most important processing techniques. Reprinted from [9] with permission of Elsevier

polymers will even become amorphous at a specific cooling rate, e.g., poly-L-lactic acid (PLLA), polyethylene terephthalate (PET), etc. Others, like LPE, are very difficult or impossible to amorphize, and one needs a fast scanning (chip) calorimeter, operating at much higher scan rates, e.g., up to 10^6 °Cs^{-1} [16], to create a chance for amorphization, as it has been done for PP [19] and PA6 [20].

Reorganization phenomena

Polymer scientists are familiar with phenomena related to metastability like supercooling, amorphization, cold crystallization, recrystallization (after melting) and remelting, annealing, etc. Figure 3 presents a striking example of the benefits of enabling a high cooling rate: cooling at a standard rate of 10 °C min^{-1} of an LLDPE/LDPE blend gives rise to a double exotherm in the DSC curve. The possibility of having two separate crystallization processes at some cooling stage during film blowing points to a possible risk of occurrence of demixing phenomena,

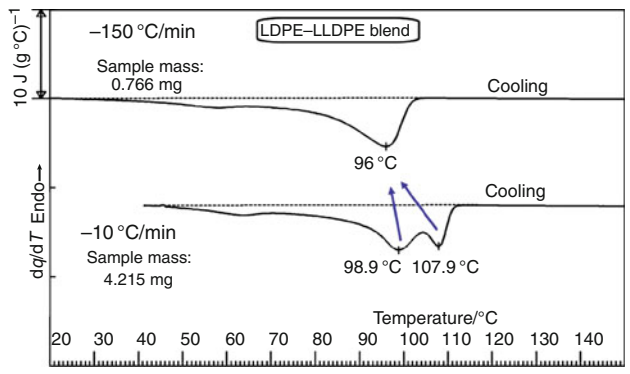

Fig. 3 Cooling at 10 °C min^{-1} gives a double-peaked DSC cooling curve, cooling at 150 °C min^{-1} in a single-peaked DSC curve. Reprinted from [9] with permission of Elsevier

leading to heterogeneities, gels, etc., causing all kinds of problems of mechanical and optical nature. However, from the measurement at a higher cooling rate of 150 °C min^{-1}, resulting in a *single* DSC peak it is obvious that at such a cooling rate cocrystallization occurs by which the risk of demixing is negligible. It is clear for this case that the standard way of measuring at −10 °C min^{-1} would steer the film blowing process into a wrong direction with possible economic consequences.

Although usually by HPer DSC one is able to suppress recrystallization, reorganization processes in general are extremely difficult to suppress. Figure 4 shows an example. Cooling at different rates—here at 1 and 150 °C min^{-1}—is not reflected in the heating curves at 150 °C min^{-1}, contrary to expectation, because one would argue that cooling at 1 °C min^{-1} would result in crystallites having larger dimensions and less imperfect structures compared to cooling at 150 °C min^{-1}. This is expected to shift (part of) the heating curve to higher temperatures.

However, as can be seen, the two heating curves are virtually identical. Obviously, during heating the fast cooled sample is vulnerable to extensive reorganization shifting the melting point distribution to higher temperatures. This implies that in such case, by measuring a heating curve of a sample "as received" the thermal history cannot be revealed. As a consequence, for this copolymer sampling of slow/fast cooled parts, like present in a core/skin product, respectively, resulting from processing, would give the same results. Here one is tempted to use the fast scanning chip calorimeter in order to discriminate the samples also in heating according to the different cooling histories [20].

Cross fractionation by the SEC-LC transform-DSC combination

In addition to studying metastability, among the many advantages of HPer DSC, measuring on minute amounts—down to the microgram level—of materials, like yields of fractionations, is possible because of the increased sensitivity provided by the high scan rates,

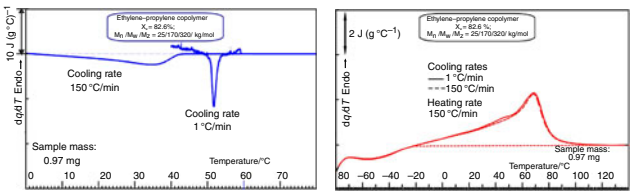

Fig. 4 Cooling at different rates of an ethylene–propylene copolymer giving drastic differences with respect to crystallization (*left*) but subsequent heating curves (*right*) at the same rate show similar melting. Reprinted from [9] with permission of Elsevier

A topic studied recently by HPer DSC addresses an issue of high importance for industry: the distribution of short chain branching (SCB) across the molar mass distribution (MMD) for bimodal HDPE grades. It is well known that the specific SCB distribution (SCBD) along the MMD determines the crystallization behavior and by that the end properties. However, the mechanisms are still not well understood, and one of the problems inhibiting progress in this field is the lack of adequate tools for determination of the actual SCBD as a function of MMD. It has to be realized that the SCB content is extremely low, and by that very difficult to measure at the moment. Preferably, cross fractionation by SCB subsequent to MMD should be done—which is anyhow the best (unequivocal) way of starting—but it is extremely difficult to evaluate if done analytically because of the small amounts of polymer fractions; or tedious and expensive if done on a preparative scale. Therefore, almost all research reported in literature so far have been done the other way around: SCB fractionation (e.g., by TREF) followed by MMD determination (SEC), with the inherent draw back of crystallization, and its many governing parameters, being a disturbing factor already at the start of the fractionation.

Following a new route (see Fig. 5), the fractionation is performed according to MM using analytical SEC (ASEC), followed by a study of the crystallization and melting behavior of the MM fractions by (HPer) DSC instead of a subsequent, *physical* crystallizability fractionation. Evaluation of the results also provides information about possible heterogeneity of the SCBD per MM fraction, even though the interpretation can be hampered by the occurrence of cocrystallization, the influence of entanglements, etc.

Over the years, the amount of starting material for ASEC has been decreased from typically 5 mg (20 years ago) to typically 800 μg of polymer nowadays. Normally, 600–800 μg of a whole polymer on a disk is the maximum amount to be deposited. However, an HDPE is much more difficult to deposit because spraying of the low MM fractions is not precise, material gets lost sideways of the disk and high MM fractions do crystallize at the nozzle. That is why 200 μg per deposition on a disk is about the maximum for such polyethylenes at the moment. Therefore, in the present case, two separate depositions, each of 200 μg, on one disk (two spots) have been combined. At the start of this study it was anticipated that the recently developed HPer DSC could be of help, because compared with Standard DSC, HPer DSC improves the sensitivity of the measurement by its capability to realize higher cooling and heating rates. Indeed, it turned out to be feasible to measure the minute amounts of fractions resulting from ASEC [21] [A. Krumme, M. Basiura, T. Pijpers, G. Vanden Poel, L-C. Heinz, R. Brüll, V. Mathot, to be published].

As a result, Fig. 6 shows that crystallization and melting of a very high-molar mass fraction of an HDPE can clearly be studied, even though the sample mass can be as low as 13 μg as in the case shown.

Crystallization/amorphization by cooling and subsequent cold crystallization by heating

Cold crystallization after hot crystallization

A virgin PET sample usually will stay amorphous during cooling at a rate of 150 °C min^{-1}. So, when it crystallizes in cooling from the melt ("hot" crystallization), as shown in Fig. 7 to approximately 10%, most probably the nucleation density has been increased by adding nucleants and/or the molar mass has been changed, etc. For this sample, during subsequent heating, the crystallinity increases substantially by cold crystallization to more than 25%, after which it decreases again by melting.

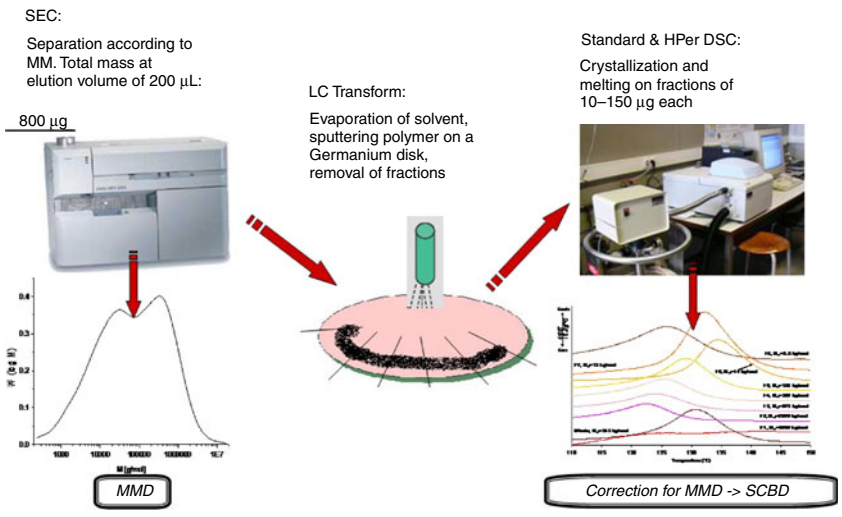

Fig. 5 The cross fractionation route followed, using the ASEC-LC Transform-DSC combination, is schematically shown: fractionation of the polymer according to MM by ASEC; subsequent deposition of the fractions on a rotating disk using a Lab Connections (LC) Transform set up; and finally off-line Standard DSC or HPer DSC on the fractions. In between, the fractions on the disk can be measured by FTIR as function of MM

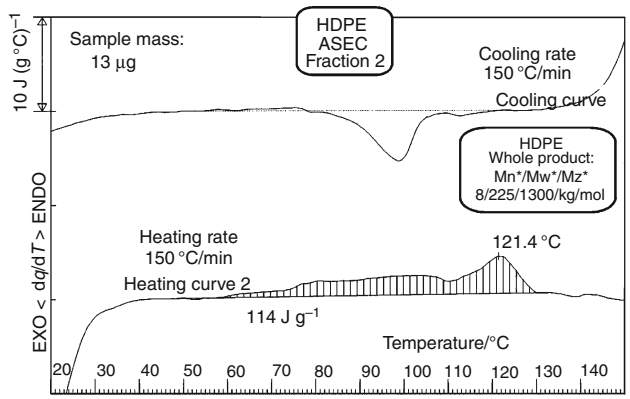

Fig. 6 HPer DSC results at 150 °C min^{-1} cooling and heating for an extremely high-molar mass fraction—ranging from 500000 to 7000000 g mol^{-1}—of a ASEC-fractionated HDPE

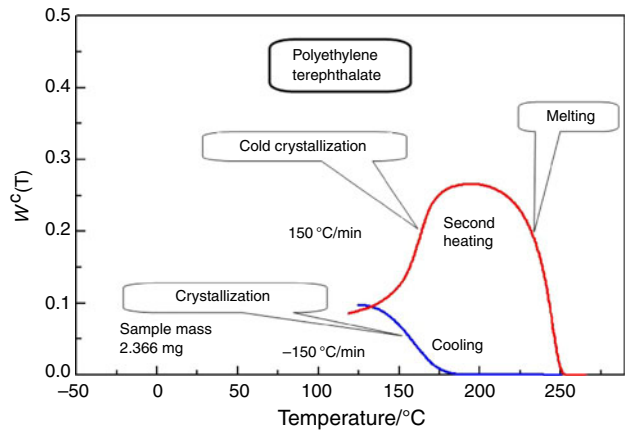

Fig. 7 An example of crystallization in two steps: hot crystallization during cooling and cold crystallization during subsequent heating, followed by final melting of the PET. Reprinted from [11] with permission of ACS

The figure illustrates that working at high scan rates in combination with low sample masses does not preclude quantitative measurements. On the contrary, the short time of measurement should suppress the influence of drift, one of the major causes of non-reproducibility of DSC measurements, resulting in less-quantitative results. In the present case a closed loop with respect to crystallinity as a function of temperature is obtained, showing the consistency of the measurements.

Cold crystallization subsequent to amorphization as influenced by nucleation density

Figure 8 (left) [22] demonstrates that normally PLLA is easy to keep in the amorphous state: even at a slow cooling rate of 5 °C min^{-1} the glass transition (or any other

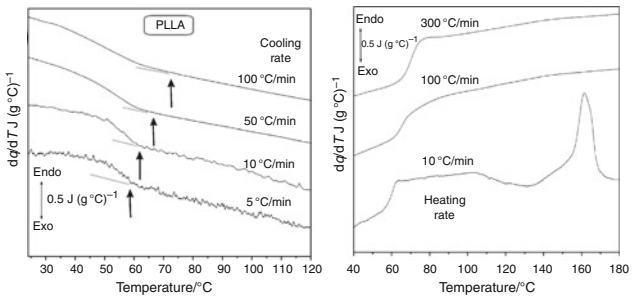

Fig. 8 (*Left*) DSC cooling curves at different rates from the melt. The *arrows* mark (somewhat arbitrary) the shift of the onset of the glass transition to higher temperatures with increasing cooling rate. (*Right*) DSC heating curves at different rates after cooling from the melt at 10 °C min^{-1}. Reprinted from [22] with permission of ACS

temperature in between T_g and the melt) can be reached without any sign of crystallization, which is confirmed by the magnitude of the step in c_p at T_g. If the sample is cooled at 10 °C min^{-1} and subsequently heated at various rates (see Fig. 8, right), cold crystallization occurs at 10 °C min^{-1} but it is effectively suppressed at the higher rates of 100 and 300 °C min^{-1}.

Thus, heating at such high rates clearly eliminates cold crystallization and as a result the heating curve reflects the preceding cooling scan, i.e., is a reflection of an amorphous sample. These results show that it is possible, coming from the glass in an amorphous state, to reach any temperature between T_g and the melt while keeping the sample in an amorphous state. In this way isothermal crystallization at a specific temperature coming either from the melt ('hot' crystallization) or from the cold side ('cold' crystallization; from below or above the glass transition) is possible.

Very peculiar is the observation that, although the samples stay amorphous during cooling at rates of 5, 10, 50, 100, and 300 °C min^{-1} into the glass, the subsequent isothermal (cold) crystallization curves at e.g., 100 °C are quite different (see Fig. 9, right). It most probably means that—depending on the cooling rate—more or less nuclei become activated during cooling though they do not give rise (yet) to crystal growth. However, when there is enough time for growth—as during the isothermal waiting time—it will happen nevertheless. Thus, cooling at lower rates results in a higher activity of nuclei compared to samples cooled at higher rates; the cooling rate modulates the number of active nuclei formed when the glass state is reached, while all nuclei can become active in time during subsequent isothermal crystallization (Fig. 9, left) or in heating, resulting in the same final morphology. Recently this concept has been confirmed for polycaprolactone using a fast scanning (chip) calorimeter [23].

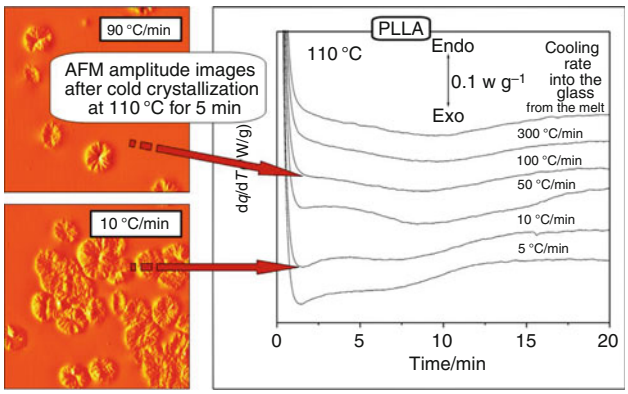

Fig. 9 (*Right*) Isothermal cold crystallization at 110 °C for 60 min (only the time span is shown in which the DSC curves show a changing heat flow rate signal) after heating from the glass state. (*Left*) Variation in activated nuclei by AFM dependent on the previous cooling rate. The sample was previously cooled at different rates (shown at each curve) from the melt into the glass state. Reprinted from [22] with permission of ACS

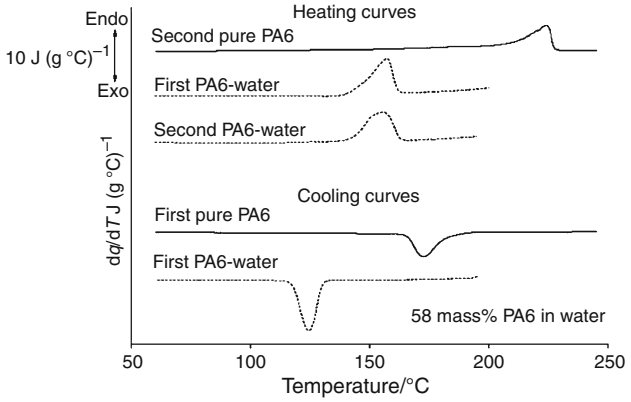

Fig. 10 Full dissolution of PA6 in water, using a hermetic closed DSC pan, during the first heating at 5 °C min^{-1}, and lowered transition temperatures in subsequent cooling and heating. Reprinted from [25] with permission of Springer

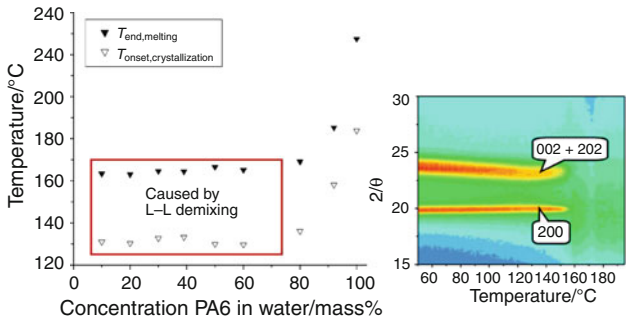

Fig. 11 (*Left*) Phase diagram of PA6 in water showing the independency of the transition temperatures in the 10–70 mass% PA6-in-water range and the maximum supercooling of approximately 60 °C. (*Right*) Time-resolved WAXD pattern during the second heating of 49 mass% PA6 in water, as function of temperature. All scanning rates were 5 °C min^{-1}

Water: from a nuisance to a prospect of utilization

Fast and full dissolution of PAs in water

Based on a study done at DSM in the 1990s [24], research has been performed [25, 26] into the full dissolution of PAs, like PA6; PA6.6 and PA4.6, in water and in other solvents like methanol, ethanol, butanol, etc. Usually water is seen as a problem for PAs because water uptake by the PA can cause blistering in electronic components. However, it turned out that if the water is kept in its liquid state also at higher temperatures, it acts as a very effective solvent. Such liquid state can be realized under pressure using an autoclave, an extruder, or on a small-scale simply by using a hermetic closed pan, like the stainless-steel high-pressure pans for DSC.

Figure 10 shows that dissolution is fast and can be realized during the first heating by DSC, without any stirring. Measurements reveal a lowering of the crystallization and melting temperatures of approximately 60 °C: 130 and 165 °C for PA6 in water compared to 184 and 227 °C for pure PA6 for onset crystallization and end melting, respectively. In case of PA4.6, the solvent-induced depression of the transition temperatures is even higher: 100 °C in water and 80 °C in methanol and ethanol. The fact that the depression is independent of the concentration over a large range, 10–70 mass% for PA6 in water (see Fig. 11, left) is in line with an upper critical temperature liquid–liquid demixing, which has been confirmed by optical measurements.

The synchrotron time-resolved WAXD measurements reveal a pattern at room temperature that displays two sharp peaks, at $2\theta = 19.6°$ [$\alpha_1(200)$] and at $2\theta = 24.0°$ [$\alpha_2(002) + (202)$] on top of a halo due to water and non-crystalline PA6. These sharp peaks point to the α-structure. When the mixture is heated at 5 °C min^{-1} (Fig. 11, right), the position of the (200) reflection (related to an intra-hydrogen-bonded sheet distance) remains almost identical, whereas the position of the (002) + (202) reflection (corresponding to the inter-hydrogen-bonded sheet distance) shifts to lower angles. This behavior is characteristic for PA6. At approximately 165 °C, the PA6 dissolves in water, in agreement with the DSC results, and accordingly the halo amplifies. Also the synchrotron time-resolved SAXS experiments confirm the DSC results. A detailed analysis of the X-ray measurements and additional calculations of possible void volumes learns that the water is located within the amorphous regions and does not enter the crystallites. Also it appears that the mobility of the chains is enhanced by the water, which is probably caused by weakening and breaking of hydrogen bonds by water uptake. This also explains that crystallization in water

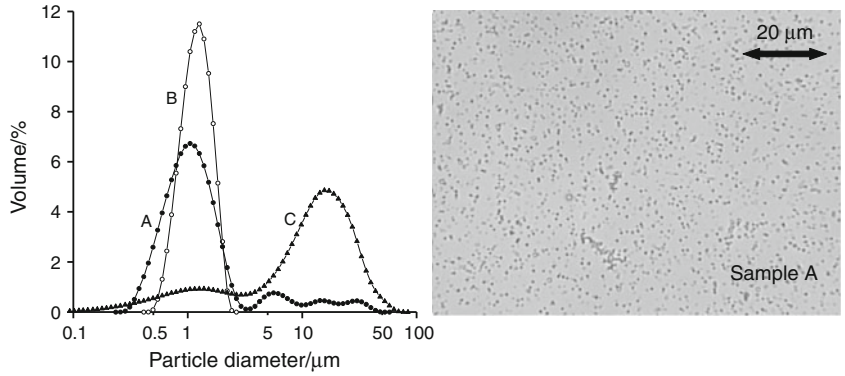

Fig. 12 Optical microscopy picture of EO copolymer droplets dispersed in water and the PSD as obtained with a Coulter LS230

increases the DSC crystallinity significantly to approximately 39%, compared with approximately 27% for pure PA6.

EO copolymer and PP droplet dispersions in water: small events on a big scale

Heterogeneous-, fractionated-, and homogeneous nucleation in case of polymer blends and composites have become topics for research linking up with studies on confined crystallization. Semicrystalline polymers generally crystallize through heterogeneous nucleation on impurities (catalyst residues, additives, processing aids, etc.) or foreign surfaces (e.g., a mold) that act as nucleation substrates.

In case of dispersions of particles in a matrix, particles having large sizes with many seeds crystallize at the common bulk crystallization temperature. However, if the polymer is dispersed into a larger amount of smaller particles, then part of them may be free of the most active seeds, giving rise to *fractionated* crystallization at some extra degree of supercooling.

In case their nucleation is not triggered at all by a foreign active surface, crystallization via *homogeneous* nucleation will occur at an even larger supercooling. As suggested, one of the available routes—besides quenching and fast cooling using a fast scanning (chip) calorimeter—to realize homogeneous nucleation is minimizing the volume for the polymer molecules by realizing many particles, toward the point where most or all of the particles do not contain seeds anymore. Thus, homogenous nucleation and crystallization at much lower temperatures than usual are realized typically by the way of making sub-micrometer-sized dispersions.

Many droplet-in-matrix systems have been obtained by melt blending of a polymer with another polymer [27]. Here, an example is given of fractionated and homogeneous nucleation of dispersions of crystallizable polyolefins in water as the matrix [28, 29]. Water has been selected for various reasons. Firstly, since water is highly polar and the polymers used in this work are completely apolar, it minimizes the possibility of any influence of the matrix on the crystallization behavior of the dispersed polymer, which has been observed for other low-molar mass matrices. Secondly, until now, water has not shown to be of much use for e.g., polyolefins. Therefore—water being an abundant and natural source and from an environmental point of view—it would be of great advantage if it could lead to any application.

Thus, very stable and high-solid water-borne dispersions of homogeneous EO copolymers (Fig. 12) and of maleic anhydride-grafted polypropylene (MA-*g*-PP) (Fig. 13) have been prepared in a controlled way on a big scale, including particles having sizes down to sub-micrometer scale. A study of crystallization of the dispersed particles by DSC reveals a correlation between particle size distribution (PSD) and crystallization mode. Dispersions of PP-*g*-MA of sizes from 100 to 200 µm down to sizes below 0.04 µm have been produced. The PSD in Fig. 12 shows only an extremely small part (2%) of the sample because particles having a size <0.04 µm are not detected by the

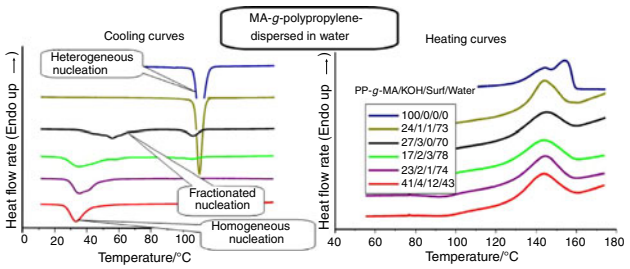

Fig. 13 DSC cooling (*left*) and subsequent heating (*right*) curves of bulk MA-*g*-PP and of MA-*g*-PP-dispersed-in-water samples showing (from top to bottom) heterogeneous, fractionated, and probably homogeneous crystallization under confined conditions, respectively. The compositions of the samples are included as mass percentages polymer/KOH/surfactant/water. Reprinted from [28] with permission of Elsevier

instrument used. Figure 13 presents the DSC cooling curves of samples, arranged in order of decreasing particle size (from top to bottom), showing a tendency of crystallization according to, respectively, heterogeneous, via fractionated toward homogeneous modes, and mixtures thereof. Thus, it is observed that the smaller the particles, the smaller the fraction of polymer molecules nucleating heterogeneously, and the larger the amount of polymer material crystallizing at lowered temperatures. The lowest crystallization peak temperature found in these experiments, 33 °C for the sample at the bottom of the Fig. 13 left, is lower than any other previously reported value in literature for PP in similar conditions, and possibly reflects homogeneous nucleation. Because the crystallization peak temperature of the bulk MA-*g*-PP used here is 110 °C, the supercooling realized is approximately 77 °C.

Compared to the cooling curves, the heating curves vary much less for all dispersions, except for the difference seen with respect to the double melting behavior of the bulk polymer and the single melting behavior of the dispersions. Thus, the high-temperature properties are preserved for all dispersions, irrespective of the crystallization mode, by reorganization phenomena.

PA6-dispersed-in-EO copolymer matrix: improved temperature resistance of the matrix

EO copolymers in which a PA6 phase is finely dispersed by means of compatibilization using grafted maleic anhydride in a polyethylene chain, PE-*g*-MA, have been studied. The droplet size distribution is reflected in the DSC curves as expected, while the resulting fractionated crystallization behavior of dispersed PA6 droplets has already been studied using different amorphous materials as matrix.

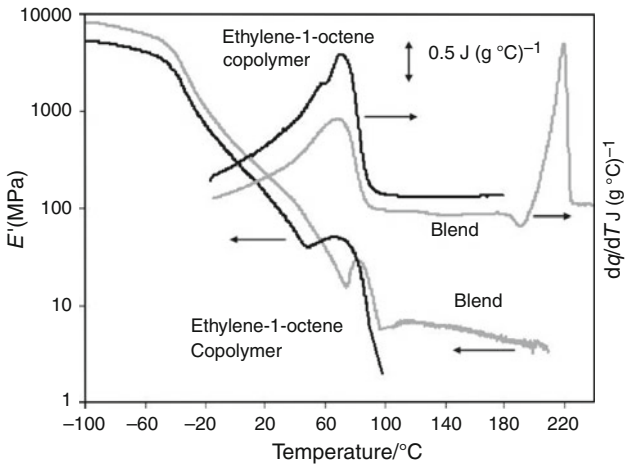

Fig. 14 Dynamic storage modulus (E') and DSC curves in heating for an EO copolymer and for an EO copolymer/PA6/compatibilizer blend (62.5 mass%/30 mass%/7.5 mass%). Reprinted from [31] with permission of Wiley

Typical effects associated to crystallization in droplets such as a decrease in crystallinity occur, while, due to the fine dispersion of the PA6, fractionated/homogeneous crystallization takes place, resulting in an extra supercooling of around 50 °C compared to the PA6 bulk crystallization temperature. The lower crystallinity in the dispersed system is probably caused by hindered crystallization due to confinement, leading to cold crystallization in subsequent heating. What makes this system peculiar is that, firstly, at room temperature the matrix is not amorphous but semi-crystalline. Secondly, the crystallization process of the dispersed phase takes place when the matrix is still in the melt state what prevents crystallization of the PA6 droplets via nucleation induced by solidification of the matrix, and thirdly, the mechanical properties of the matrix are improved much more than expected.

Figure 14 shows the storage modulus (E') and the DSC curves in heating for the EO copolymer used and for the blend: PA6-dispersed-in-EO matrix [30, 31]. The modulus of the pure EO copolymer drops above 100 °C, once the irreversible flow of the polymer chains starts in the melt state, which is expected for a system that is not chemically crosslinked. Thus, it is no longer possible to measure the tensile mechanical modulus with the DMTA apparatus because of the macroscopically fast flow of the sample.

For the blend, up to 100 °C, the storage modulus is quite similar to that of the EO copolymer. However, once the matrix is molten, see the corresponding DSC curve, the storage modulus *still keeps its value*, which is quite exceptional. This behavior continues till the main melting of the dispersed PA6 starts. The measured E' values (higher than 1 MPa) above the melting point of the matrix are approximately comparable to those of crosslinked elastomers. This high-temperature behavior is not expected at all for a 'normal' blend with dispersed droplet morphology: one would expect no connections between the PA6 particles, and at temperatures above the melting range of the matrix the modulus should drop because of flow of chains in the melt. Instead, it is even possible to measure the tensile modulus of the blend up to 200 °C, that is, until the melting of the dispersed PA6 droplets starts. It turns out that at the same time, the system shows dimensional stability.

The explanation of this high-temperature effect comes from the architecture of the molecular system and is found in a slowed-down flow dynamics of the EO matrix chains. The mixing and interactions of these chains with the compatibilizer chains increases the entanglement density. While the compatibilizer chains are connected to the droplets, these function as physical crosslinks. The intriguing behavior of this system at higher temperatures, resulting in improved mechanical properties compared to what would be expected for a conventional blend having

the (qualitatively) same morphology and composition, allows extending the use of the EO copolymer to applications for which dimensional stability is required at high temperatures.

Acknowledgements The lifetime collaboration with my colleagues, and especially with M. (Thijs) F. J. Pijpers, is much appreciated. Support for SciTe from the FP7 CSA project "NaPolyNet," see www.napolynet.eu, is valued.

References

1. Mathot VBF. The crystallization and melting region. In: Mathot VBF, editor. Calorimetry and thermal analysis of polymers, chap. 9. New York: Hanser Publishers; 1994. p. 231–99.
2. Mathot VBF. Temperature dependence of some thermodynamic functions for amorphous and semi-crystalline polymers. Polymer. 1984;25:579–99. Errata: Polymer 1986;27:969.
3. Mathot VBF. Thermal characterization of states of matter. In: Mathot VBF, editor. Calorimetry and thermal analysis of polymers, chap. 5. New York: Hanser Publishers; 1994. p. 105–67.
4. Mathot VBF. A lifetime in research, NATAS notes 42(2,3). Spring, Summer, 2009. p. 9–16.
5. Mathot VBF, editor. Thermal analysis and calorimetry in polymer physics. Thermochim Acta. 1994;238(special issue), 459 pp.
6. Mathot VBF. Thermal analysis and calorimetry beyond 2000: challenges and new routes. Thermochim Acta. 2000;355:1–33.
7. Mathot VBF. New routes for thermal analysis and calorimetry as applied to polymeric systems. J Thermal Anal Calorim. 2001;64:15–35.
8. Mathot VBF, Reynaers H. Crystallization, melting and morphology of homogeneous copolymers. In: Cheng SZD, editor. Handbook of thermal analysis and calorimetry: applications to polymers and plastics, vol. 3, chap. 6. Elsevier Science; 2002. p. 197–244.
9. Mathot VBF, Vanden Poel G, Pijpers TFJ. Benefits and potentials of high performance differential scanning calorimetry (HPer DSC). In: Brown ME, Gallagher PK, editors. Handbook of thermal analysis and calorimetry: recent advances, techniques and applications, vol. 5, chap. 8. Elsevier Science; 2008. p. 269–97.
10. See www.scite.eu for references and more information. SciTe is member of evitherm (www.evitherm.org) and NaPolyNet (www.napolynet.eu).
11. Pijpers MFJ, Mathot VBF, Goderis B, Scherrenberg RL, van der Vegte EW. High-speed calorimetry for the study of the kinetics of (De)vitrification, crystallization, and melting of macromolecules. Macromolecules. 2002;35(9):3601–13.
12. Mathot VBF, Vanden Poel G, Pijpers TF. Improving and speeding up the characterization of substances, materials, and products: Benefits and potentials of high-speed DSC. Am Lab. 2006;38(14):21–5. www.scite.eu.
13. See www.scite.eu and also the webcasts by Mathot VBF, downloadable for free through this website.
14. See the website of PerkinElmer: www.hyperdsc.com.
15. Danley RL, Caulfield PA, Aubuchon SR. A rapid-scanning differential scanning calorimeter. Am Lab. 2008;40(1):9–11.
16. Efremov MY, Olson EA, Zhang M, Lai SL, Schiettekatte F, Zhang ZS, Allen LH. Thin-film differential scanning nanocalorimetry: heat capacity analysis. Thermochim Acta. 2004;412:13–23.
17. Minakov AA, Schick C. Ultrafast thermal processing and nanocalorimetry at heating and cooling rates up to 1 MKs^{-1}. Rev Sci Instrum. 2007;78(7):art. no. 073902.
18. Vanden Poel G, Mathot VBF. High performance differential scanning calorimetry (HPer DSC): a powerful analytical tool for the study of the metastability of polymers. Thermochim Acta. 2007;461(1–2):107–21.
19. Mileva D, Androsch R, Zhuravlev E, Schick C. Critical rate of cooling for suppression of crystallization in random copolymers of propylene with ethylene and 1-butene. Thermochim Acta. 2009;492(1–2):67–72.
20. Tol RT, Minakov AA, Adamovsky SA, Mathot VBF, Schick C. Metastability of polymer crystallites formed at low temperature studied by ultra fast calorimetry: polyamide 6 confined in submicrometer droplets vs bulk PA6. Polymer. 2006;47(6):2172–8.
21. Luruli N, Pijpers T, Brüll R, Grumel V, Pasch H, Mathot V. Fractionation of ethylene/1-pentene copolymers using a combination of SEC-FTIR and SEC-HPer DSC. J Polym Sci B Polym Phys. 2007;45(21):2956–65.
22. Salmerón Sánchez M, Mathot VBF, Vanden Poel G, Gómez Ribelles JL. Effect of the cooling rate on the nucleation kinetics of poly(l-lactic acid) and its influence on morphology. Macromolecules. 2007;40:7989–97.
23. Zhuravlev E, Schick C. Nucleation formation in PCL in a wide range of time and temperature studied by fast scanning calorimetry. Abstracts NATAS Conference, September 20–23, 2009. Lubbock, Texas, USA, p. 195.
24. Pijpers MFJ, Mathot VBF, Scherrenberg RL. Kristallisatie- en smelttemperatuur depressie van polyamiden door water, methanol and andere oplosmiddelen onder verhoogde (damp)druk. Technical Report RC95-12799. DSM Research; 1995.
25. Wevers M. Full dissolution and crystallization of polyamides in water and other solvents. PhD thesis, Katholieke Universiteit Leuven, Belgium; 2006. 220 pp, ISBN 978-90-8649-070-7.
26. Wevers MGM, Mathot VBF, Pijpers M, Goderis B, Groeninckx G. Full dissolution and crystallization of PA6 and Polyamide 4.6 in water and ethanol. In: Reiter G, Strobl G, editors. Lecture Notes in Physis, vol. 714. Berlin/Heidelberg: Springer; 2007. p. 151–68.
27. See www.scite.eu for references of publications by Homminga D, Groeninckx G, Tol R.
28. Ibarretxe Uriguen J, Bremer L, Mathot V, Groeninckx G. Preparation of water-borne dispersions of polyolefins: new systems for the study of homogeneous nucleation of polymers. Polymer. 2004;45(17):5961–8.
29. Ibarretxe Uriguen J, Groeninckx G, Bremer L, Mathot VBF. Quantitative evaluation of fractionated and homogeneous nucleation of polydisperse distributions of water-dispersed maleic anhydride-grafted-polypropylene micro- and nano-sized droplets. Polymer. 2009;50(19):4584–95.
30. Salmerón Sánchez M, Mathot V, Groeninckx G, Bruls W. Submicrometer polyamide droplets dispersed in polyethylene: dimensional stability above the melting point of polyethylene. Polymer. 2006;47(15):5314–22.
31. Salmerón Sánchez M, Mathot V, Vanden Poel G, Groeninckx G, Bruls W. Crystallization of polyamide confined in sub-micrometer droplets dispersed in a molten polyethylene matrix. J Polym Sci B Polym Phys. 2006;44(5):815–25.